Time-reversal symmetry breaking in s-wave superconductor $CaPd_2As_2$ probed by μSR

Aarti,[1] K. Panda,[2] D. T. Adroja,[3,4] A. Bhattacharyya,[5,*] P. K. Biswas,[3,†]
A. D. Hillier,[3] B. Lake,[6] Samar Layek,[1] and V. K. Anand[1,6,7,8,‡]

[1]*Department of Physics, University of Petroleum and Energy Studies, Dehradun, Uttarakhand, 248007, India*
[2]*Department of Physics, Ariel University, Ariel 40700, Israel*
[3]*ISIS Facility, Rutherford Appleton Laboratory, Chilton, Didcot, Oxon, OX11 0QX, United Kingdom*
[4]*Highly Correlated Matter Research Group, Physics Department, University of Johannesburg, P.O. Box 524, Auckland Park 2006, South Africa*
[5]*Department of Physics, Ramakrishna Mission Vivekananda Educational and Research Institute, Belur Math, Howrah 711202, West Bengal, India*
[6]*Helmholtz-Zentrum Berlin für Materialien und Energie GmbH, Hahn-Meitner Platz 1, D-14109 Berlin, Germany*
[7]*Department of Mathematics and Physics, University of Stavanger, 4036 Stavanger, Norway*
[8]*Department of Physics, National Institute of Technology Agartala, Tripura 799046, India*

(Dated: December 21, 2024)

$CaPd_2As_2$ is known to superconduct below $T_c = 1.27(3)$ K. In this work we examine whether the time-reversal symmetry (TRS) is preserved or broken upon entering the superconducting state in $CaPd_2As_2$, and probe its superconducting gap structure using muon spin relaxation and rotation (μSR) measurements in zero-field (ZF) and transverse-field (TF), respectively. The analysis of ZF-μSR spectra reveals an increase in muon spin relaxation rate λ_{ZF} in the superconducting (SC) state attesting the presence of a weak magnetic field. The appearance of spontaneous magnetic field indicates the breaking of time reversal symmetry state upon entering the SC state of $CaPd_2As_2$. The analysis of TF-μSR spectra provides information about the superconducting gap structure of $CaPd_2As_2$ which is found to have a single-band isotropic s-wave symmetry. We find an isotropic energy gap $\Delta(0) = 0.160(1)$ meV corresponding to $2\Delta(0)/k_BT_c = 3.37(3)$ which is close to the weak coupling BCS value of 3.53. The analysis of TF-μSR also provides an estimate of effective penetration depth which is found to be $\lambda_{eff}(0) = 415(16)$ nm. Our μSR data thus find evidence for TRS breaking in $CaPd_2As_2$ with a s-wave singlet paring which is not expected for a conventional superconductor.

I. INTRODUCTION

Recently an increasing number of superconductors have been found to exhibit time-reversal symmetry (TRS) breaking [1–24]. Within the framework of BCS theory of conventional superconductors, the occurrence of superconductivity is understood in terms of spontaneously broken global $U(1)$ gauge symmetry upon the formation of Cooper pairs below a critical temperature T_c. However, there are some superconductors which break time reversal symmetry in addition to $U(1)$ gauge symmetry. The TRS broken state is characterized by the spontaneous appearance of a weak magnetic field in superconducting state. The muon spin relaxation and rotation (μSR) technique proves to be a very useful tool for probing the time reversal symmetry state of a superconductor. Sr_2RuO_4 [3, 25–27] characterized by an odd-parity chiral p-wave symmetry ($p_x \pm ip_y$) order parameter is a well-known example for which μSR detects the spontaneous weak magnetic field upon entering the superconducting state on account of TRS breaking. SrPtAs is another example of TRS broken superconductor for which the order parameter is characterized by a chiral d-wave symmetry ($d + id$) [9]. $LaNiC_2$ is found to exhibit TRS breaking with possible triplet paring on account of the lack of a crystallographic inversion symmetry [10]. The TRS breaking in these systems might arise due to a non-unitary triplet pairing state or a mixed singlet-triplet state. A recent review by Ghosh *et al.* can be of interest for more details on theoretical and experimental aspects of TRS breaking [1].

The μSR investigations have provided evidence for TRS breaking in several nodeless full-gap superconducting materials, to mention some of them: $A_5Rh_6Sn_{18}$ (A = Y, R, or Sc) [11–13], $La_7(Ir, Rh, Pd)_3$ [14–16], Re_6X (X = Zr, Hf and Ti) [5–8], and Zr_3Ir [17]. For $A_5Rh_6Sn_{18}$ (A = Y, R, or Sc) a multi-component singlet or triplet order parameter is proposed to explain TRS breaking [1]. For $La_7(Ir, Rh, Pd)_3$ and Zr_3Ir the order parameter is proposed to be a singlet dominated mixed-state [1]. In the case of Re_6X (X = Zr, Hf and Ti) for which crystal symmetry allows the formation of microscopic super-current loops, a model based on loop super-current order has been proposed to explain the TRS breaking [1, 2]. In the case of a multi-band superconductor, the development of a complex gap structure due to the inter-band interactions can cause a TRS breaking [28]. While the TRS breaking in unconventional and multiband superconductors have been discussed and understood up to a certain extent, the TRS breaking in a conventional electron-phonon mediated single-band s-wave superconductor with a nodeless isotropic gap structure lacks theoretical understanding, and invites further

* amitava.bhattacharyya@rkmvu.ac.in
† Deceased.
‡ vivekkranand@gmail.com

research. $Sc_5Co_4Si_{10}$ [19] and $CaPd_2Ge_2$ [20] are two such single-band s-wave TRS broken superconductors recently investigated by some of us.

In our efforts to understand the possible mechanism behind TRS breaking in single-band s-wave superconductor, some of us examined the symmetry allowed pairing states in $Sc_5Co_4Si_{10}$ which negated the presence of non-unitary or mixed singlet-triplet state [19]. Theoretical considerations suggest that TRS breaking by conventional electron-phonon mechanism can be possible for certain specific Fermi surface topography [19]. Very recently, through our μSR study we found evidence for TRS breaking in $CaPd_2Ge_2$ [20]. $CaPd_2Ge_2$ forms in a centrosymmetric $ThCr_2Si_2$-type body-centered tetragonal structure (space group $I4/mmm$) and exhibits superconductivity below $T_c \sim 1.7$ K [29]. Finding of TRS breaking in single-band isotropic s-wave superconductor $CaPd_2Ge_2$ motivated us to investigate the superconducting gap structure and time reversal symmetry state of the related compound $CaPd_2As_2$.

$CaPd_2As_2$ adopts a $ThCr_2Si_2$-type body-centered tetragonal structure (space group $I4/mmm$) and exhibits superconductivity below $T_c = 1.27(3)$ K [30]. The temperature T dependence of the superconducting state electronic heat capacity C_e of single crystal $CaPd_2As_2$ has been found to yield a reduced value of jump ΔC_e at T_c with $\Delta C_e/\gamma_n T_c \approx 1.14$ (BCS theory predicted value is 1.43) [30]. An analysis of superconducting state $C_e(T)$ data of $CaPd_2As_2$ within the framework of the α-model of BCS superconductivity [31, 32] suggests that the $C_e(T)$ data are well described by $\alpha = \Delta(0)/k_B T_c = 1.58$ instead of the the BCS expected value $\alpha_{BCS} = 1.764$ [30]. The reduced value of α and $\Delta C_e/\gamma_n T_c$ despite sharp superconducting transition in single crystalline sample of $CaPd_2As_2$, which is thought of to be free of non-superconducting impurity contributions, could be caused by the presence of weak anisotropy in superconducting gap structure [32]. A similar reduced values of $\alpha = 1.62$ and $\Delta C_e/\gamma_n T_c = 1.21$ were found in the case of single crystal $CaPd_2Ge_2$ [29], however the μSR measurement [20] revealed a fully gapped isotropic s-wave superconductivity in this compound. The nuclear magnetic resonance (NMR) and nuclear quadrupole resonance (NQR) measurements on single crystal $CaPd_2As_2$ revealed a fully gapped conventional s-wave superconductivity [33]. The NMR-NQR measurements also revealed the observation of Volovik effect in $CaPd_2As_2$ which is not expected in nodeless s-wave superconductors [33].

The band structure calculations within the local density approximation [34] and the first principles calculations by means of the full-potential method [35] reveal that $CaPd_2As_2$ has a three-dimensional Fermi-surface. The electronic structure calculations find the bare (band structure) density of states at the Fermi level $\mathcal{D}_{Band}(E_F) = 1.865$ states/(eV f.u.) [35] in very good agreement with the experimental value of 1.87(1) states/(eV f.u.) estimated from the analysis of the heat capacity [30]. The electronic structure calculations show that major contributions to $\mathcal{D}_{Band}(E_F)$ come from Pd $4d$ and As $4p$ states (with almost negligible contribution from Ca) [34, 35]. Further, the electronic structure calculations also reveal strong hybridization between these Pd $4d$ and As $4p$ states [34, 35], which is consistent with the collapsed tetragonal structure of $CaPd_2As_2$ [30, 36].

In this work we report the results of our μSR study on $CaPd_2As_2$ which confirm a single-gap isotropic s-wave superconductivity but with a broken time-reversal symmetry in the superconducting state. As outlined above, the TRS breaking in a conventional electron-phonon mediated single-band superconductor $CaPd_2As_2$ with an isotropic gap structure and a s-wave singlet paring is very exciting as well as mystifying.

II. EXPERIMENTAL

A polycrystalline sample of $CaPd_2As_2$ was synthesized by combining the high-purity elements from Alfa Aesar [Ca-99.98%, Pd-99.95%, As-99.999%] through the standard solid-state reaction method at the Core Lab for Quantum Materials, Helmholtz-Zentrum Berlin (HZB). The synthesis procedure is very similar to that of the $CaPd_2Ge_2$ [20]. Pelletized Ca pieces and Pd and As powders were sealed in an evacuated quartz tube and heat treated at 800 °C for 30 hours, after which it was finely ground, pelletized and sealed in quartz tube again following a firing at 900 °C for 72 hours. The sequence of grinding, pelletizing and firing (fired at 900 °C for another 72 hours) processes were repeated again which yielded the desired single phase $CaPd_2As_2$ sample. The quality of the sample was checked using the powder x-ray diffraction measurement at room temperature using Cu-K_α radiation with a laboratory-based Bruker-D8 x-ray diffractometer. The Rietveld refinement of the XRD pattern (using FullProf [37]) confirmed the $ThCr_2Si_2$-type body-centered tetragonal structure with no spurious impurity peak. The lattice parameters $a = 4.2899(1)$ Å and $c = 10.0970(2)$ Å, and As c-axis coordinate $z_{As} = 0.3783(3)$ are found to be in good agreement with the literature values [38] and those of the single crystal $CaPd_2As_2$ [30].

The muon spin relaxation and rotation measurements were conducted at the ISIS facility, Didcot, UK, with the muon spectrometer MuSR [39], both in zero-field (ZF) and applied magnetic fields in longitudinal (referred as LF) as well as transverse geometry (referred as TF). For μSR measurement the powdered $CaPd_2As_2$ sample was placed on a high-purity Ag-plate (99.999%) with the help of diluted GE varnish which was then covered with thin silver foils. Proper measures were taken to cancel the stray fields to within the 1 μT using the correction coils. The ZF-μSR data were collected at several temperatures between 0.07 K (below T_c) and 2.4 K (above T_c). The TF-μSR data were collected between 0.04 K and 1.7 K with transverse fields of $H = 5$, 10, 20, and 30 mT. We

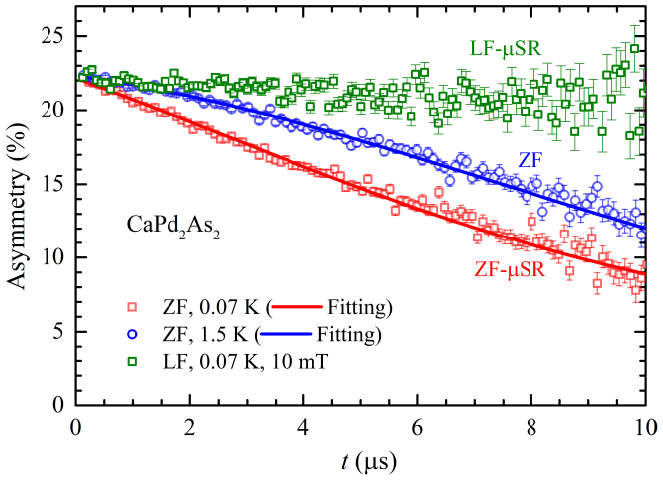

FIG. 1. Time t evolution of muon asymmetry $A_{\rm ZF}$ for representative zero-field (ZF) μSR spectra of $CaPd_2As_2$ at the temperatures 0.07 K (superconducting state) and 1.5 K (normal state). The solid lines represent the fits according to Eq. (1). The μSR spectra measured in a longitudinal field (LF) of 10 mT is also shown for comparison.

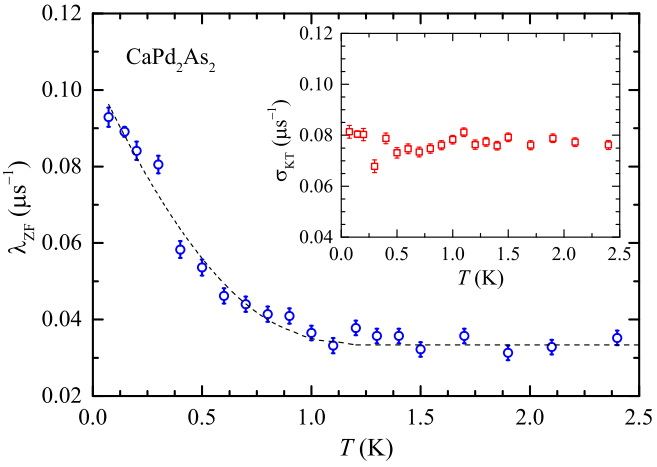

FIG. 2. Temperature T dependence of the muon spin relaxation rate $\lambda_{\rm ZF}$ obtained from the fits of zero-field μSR spectra of $CaPd_2As_2$ according to Eq. (1). The dashed line is a guide to the eye. Inset shows the T dependence of the parameter $\sigma_{\rm KT}$ in Eq. (2).

analyzed the μSR data using the program WiMDA [40].

III. RESULTS AND DISCUSSION

A. ZF μSR: Time-Reversal Symmetry Breaking

Figure 1 shows the time t evolution of muon asymmetry $A_{\rm ZF}$ spectra measured in zero-field for $CaPd_2As_2$. The $A_{\rm ZF}(t)$ spectra for representative temperatures 0.07 K ($T < T_c$, superconducting state) and 1.5 K ($T > T_c$, normal state) clearly show marked difference in their relaxation. We analyzed the $A_{\rm ZF}(t)$ spectra using a damped Gaussian Kubo-Toyabe function [41, 42].

$$A_{\rm ZF}(t) = A_0\, G_{\rm KT}(t)\, {\rm e}^{-\lambda_{\rm ZF} t} + A_{\rm BG}, \qquad (1)$$

with A_0 as the initial muon asymmetry at $t = 0$, and λ_{ZF} as the rate of muon spin relaxation in zero field. $A_{\rm BG}$ represents the non-relaxing contribution from the Ag-sample holder. The Gaussian Kubo-Toyabe term $G_{\rm KT}(t)$ is given by

$$G_{\rm KT}(t) = \left[\frac{1}{3} + \frac{2}{3}\left(1 - \sigma_{\rm KT}^2 t^2\right) {\rm e}^{-\sigma_{\rm KT}^2 t^2/2}\right] \qquad (2)$$

where $\sigma_{\rm KT} = H_\mu \gamma_\mu$ describes the Gaussian distribution of static fields H_μ due to the nuclear moments with $\gamma_\mu/2\pi = 135.53$ MHz/T, γ_μ being the muon gyromagnetic ratio.

The fits of the representative $A_{\rm ZF}(t)$ spectra by Eq. (1) are shown in Fig. 1 by the solid curves of respective colors. The T dependence of the relaxation rate obtained from the fits of the $A_{\rm ZF}(t)$ spectra for 0.07 K $\leq T \leq$ 2.4 K is shown in Fig. 2. The $\lambda_{\rm ZF}(T)$ shows a significant increase at $T < T_c$ (in the superconducting state) which indicates that the muons sense the presence of a magnetic field inside the material upon entering into the superconducting state. Thus, we notice that the muons confirm the presence of spontaneous appearance of magnetic field in superconducting state associated with the time-reversal symmetry breaking in $CaPd_2As_2$.

In order to make sure that the increase in $\lambda_{\rm ZF}$ below T_c is caused by the spontaneous static magnetic field associated with TRS breaking, and not due to the rapidly fluctuating magnetic fields on account of impurity-induced effect, we also performed μSR measurement under longitudinally applied magnetic field. We notice that a weak longitudinal field of 10 mT (see Fig. 1) is sufficient to fully decouple the muon spins from the relaxation channel associated with the spontaneous internal field. This indicates that the increased relaxation observed below T_c does not originate from rapidly fluctuating fields [43], rather is associated with very weak spontaneous fields that are static or quasistatic on the timescale of muon probing time. The appearance of spontaneous static magnetic field just below T_c, closely linked to superconductivity, provide strong evidence for a time-reversal symmetry broken superconducting state in $CaPd_2As_2$.

We see that in SC state (at 0.07 K) the $\lambda_{\rm ZF}$ is increased by 0.047(4) μs^{-1} compared to its value in normal state, which corresponds to a characteristic magnetic field $H_{\rm TRSB}$ of strength $\Delta\lambda_{\rm ZF}/\gamma_\mu = 0.055(5)$ mT. The magnitude of this characteristic field is comparable to what have been found in other TRS broken superconductors and provides clear evidence for the TRS breaking in SC state of $CaPd_2As_2$. To mention a few, the $H_{\rm TRSB} = 0.034(2)$ mT for $CaPd_2Ge_2$ [20], $H_{\rm TRSB} \approx 0.020$ mT for $Sc_5Co_4Si_{10}$ [19], $H_{\rm TRSB} \approx 0.050$ mT for Sr_2RuO_4 [25], $H_{\rm TRSB} \approx 0.006$ mT for La_7Pd_3 [15] and $H_{\rm TRSB} \approx 0.009$ mT for Zr_3Ir [17].

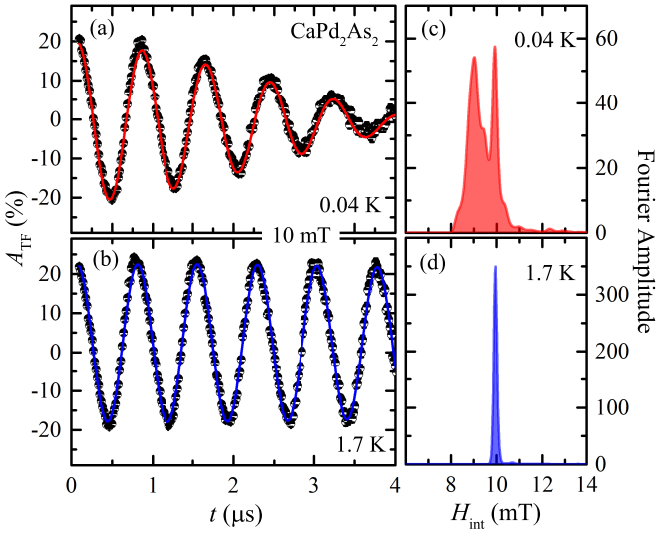

FIG. 3. Time t evolution of muon asymmetry $A_{\rm TF}$ spectra of $CaPd_2As_2$ measured in field-cooled condition in an applied transverse magnetic field $H = 10$ mT at (a) 0.04 K and (b) 1.7 K with their corresponding Fourier transformed maximum entropy spectra in (c) and (d), respectively. The solid curves in (a) and (b) represent the fits according to Eq. (3)

We also notice that the $\lambda_{\rm ZF}(T)$ of $CaPd_2As_2$ shows an unusual upward concavity, while the majority of known TRS broken superconductors show a downward concavity in $\lambda_{\rm ZF}(T)$. A similar upward concavity in $\lambda_{\rm ZF}(T)$ was also noticed in the case of $CaPd_2Ge_2$ [20]. The T dependence of $\sigma_{\rm KT}$ obtained from the analysis of the $A_{\rm ZF}(t)$ spectra of $CaPd_2As_2$, presented in the inset of Fig. 2, is nearly independent of T over 0.07 K $\leq T \leq$ 2.4 K.

B. TF μSR: Superconducting Gap Structure

Figure (3) shows the time evolution of muon asymmetry $A_{\rm TF}(t)$ spectra collected in field-cooled condition for a representative applied transverse magnetic field of $H = 10$ mT at 0.04 K and 1.7 K along with their corresponding Fourier transformed maximum entropy spectra. A comparison of TF μSR asymmetry spectra at 0.04 K ($T < T_c$) and 1.7 K ($T > T_c$) clearly show the marked difference. In the SC state there is a strong depolarization of muons as they sense an inhomogeneous field distribution due to the formation of vortex state.

We analyzed the $A_{\rm TF}(t)$ μSR spectra using a Gaussian oscillatory function with an oscillatory background [44], i.e.,

$$A_{\rm TF}(t) = A_1 \cos(\omega t + \phi)\, e^{-\sigma_{\rm TF}^2 t^2/2} + A_{\rm BG} \cos(\omega_{\rm BG} t + \phi). \quad (3)$$

Here A_1 and $A_{\rm BG}$ are the initial asymmetries of the sample and the Ag-sample holder, respectively at $t = 0$. The frequency is related to the internal field $H_{\rm int}$ at the muon site, $\omega = \gamma_\mu H_{\rm int}$, and $\omega_{\rm BG} = \gamma_\mu H_{\rm int,BG}$, and ϕ

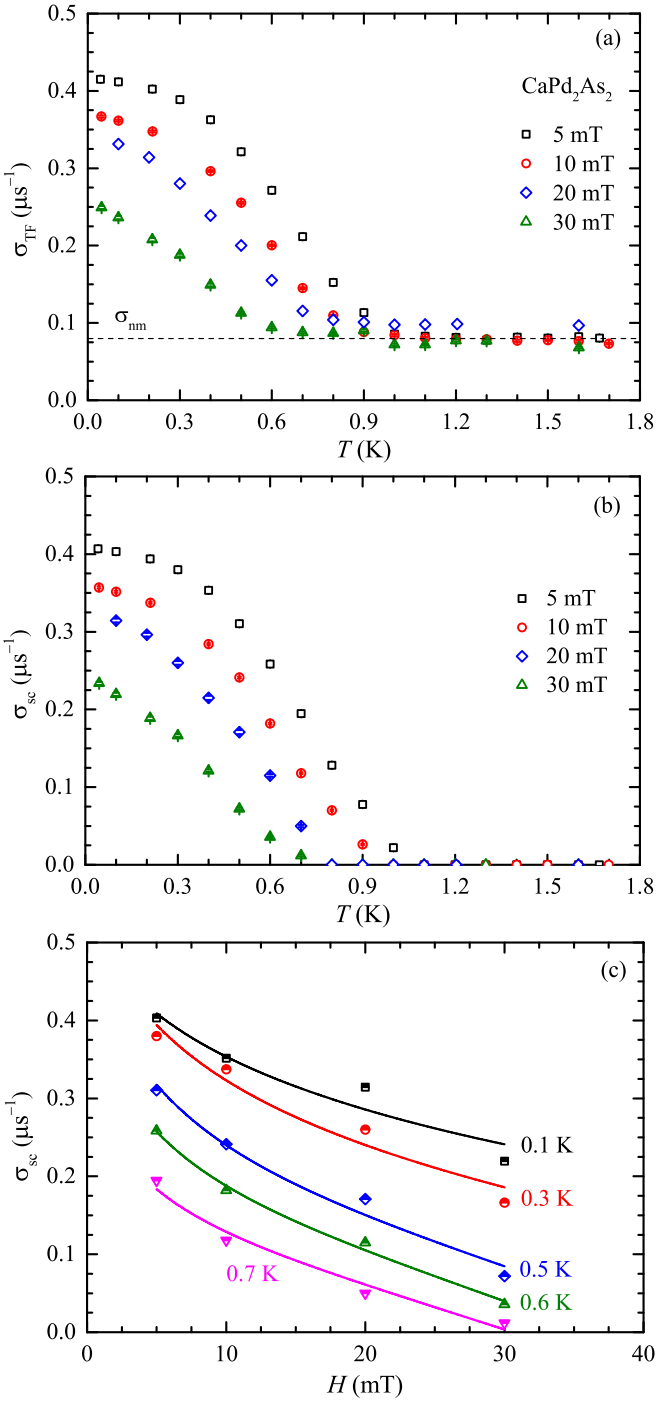

FIG. 4. (a) Temperature T dependence of muon spin relaxation rate $\sigma_{\rm TF}$ obtained from the fits of the μSR spectra of $CaPd_2As_2$ collected in field-cooled state with the indicated applied transverse magnetic fields H. (b) The superconducting contribution to muon spin relaxation rate $\sigma_{\rm sc}$ versus T. (c) The H dependence of $\sigma_{\rm sc}$ at indicated temperatures. The solid lines are the fits according to Brandt relation, Eq. (4).

is the initial phase offset. The Gaussian relaxation rate $\sigma_{\rm TF}^2 = \sigma_{\rm sc}^2 + \sigma_{\rm nm}^2$ with $\sigma_{\rm sc}$ as the superconducting contribution, accounting for the non-homogeneous field variation in the vortex state, and $\sigma_{\rm nm}$ accounting for the contribution from nuclear dipolar moments. We estimated the value of $\sigma_{\rm nm}$ by fitting the $A_{\rm TF}(t)$ spectra in normal state ($T > T_c$) which was kept fixed while fitting the $A_{\rm TF}(t)$ spectra at $T < T_c$ to isolate the value of $\sigma_{\rm sc}$.

We fitted the $A_{\rm TF}(t)$ spectra by the the function given in Eq. (3) and obtained the T dependent $\sigma_{\rm TF}$ as shown in Fig. 4(a). From $\sigma_{\rm TF}$ we determined $\sigma_{\rm sc}$, the T and H dependences of which are shown in Figs. 4 (b) and (c), respectively. The fits of the representative $A_{\rm TF}(t)$ spectra by Eq. (3) are shown by solid red and blue curves in Figs. 3 (a) and (b). It is seen from Fig. 4(a) that the value of $\sigma_{\rm TF}$ in superconducting state ($T < T_c$) is much larger than that in normal state (at $T > T_c$).

The Fourier transform of TF μSR asymmetry spectra shown in Figs. 3 (c) and (d) describes the magnetic field probability distribution which is obtained using the maximum entropy method. It is seen that there are two peaks in the superconducting state (0.04 K, $T < T_c$) and one peak in the normal state (at 1.7 $K, T > T_c$). In the SC state the first peak occurs at a field $H_{\rm int}$ equal to $H_{\rm ext}$, and the second peak occurs at $H_{\rm int} < H_{\rm ext}$. On the other hand, in normal state there is only one peak at $H_{\rm int} = H_{\rm ext}$. The additional peak in the superconducting state shows a type-II superconductivity in $CaPd_2As_2$. A type-II behavior has also been inferred from the value of Ginzburg-Landau parameter $\kappa_{GL} = 11.7 > 1/\sqrt{2}$ for $CaPd_2As_2$ [30].

Next we estimate the value of effective penetration depth $\lambda_{\rm eff}$ using the Brandt relation [45–48]

$$\sigma_{\rm sc} = \frac{4.83\times10^4}{\lambda_{\rm eff}^2}(1 - H_{\rm ext}/H_{c2}) \times [1 + 1.21\left(1 - \sqrt{(H_{\rm ext}/H_{c2})}\right)^3] \quad (4)$$

where $\sigma_{\rm sc}$ is in units of μs^{-1} and $\lambda_{\rm eff}$ in nm. For $CaPd_2As_2$, $H_{c2} = 157$ mT [30] which is much higher than the $H_{\rm ext}$ under which TF μSR spectra were collected. As such the use of Brandt relation, which is valid for $H_{\rm ext}/H_{c2} \leq 0.25$, and for $\kappa_{GL} \geq 5$ (11.7 for the present compound), is justified. The fits of $\sigma_{\rm sc}(H)$ according to Eq. (4) are shown by solid curves in Fig. 4(c). The T dependence of $\lambda_{\rm eff}$ obtained this way is presented in Fig. 5 as $\lambda_{\rm eff}^{-2}(T)/\lambda_{\rm eff}^{-2}(0)$. The $\lambda_{\rm eff}^{-2}(T)/\lambda_{\rm eff}^{-2}(0)$ data in Fig. 5 are based on all four-field sets of $\sigma_{\rm sc}(T, H)$ [see Figs. 4 (b) and (c) for clarity].

Further we extract the information about the superconducting carrier density, size and symmetry of the superconducting gap structure by analyzing the $\lambda_{\rm eff}(T)$ using the relation [24, 49, 50].

$$\frac{\sigma_{\rm sc}(T)}{\sigma_{\rm sc}(0)} = \frac{\lambda_{\rm eff}^{-2}(T,\Delta)}{\lambda_{\rm eff}^{-2}(0)} = 1 + \frac{1}{\pi}\int_0^{2\pi}\int_{\Delta(T,\varphi)}^{\infty}\frac{\partial f}{\partial E}\frac{E\,dE\,d\varphi}{\sqrt{E^2 - \Delta^2(T,\varphi)}}, \quad (5)$$

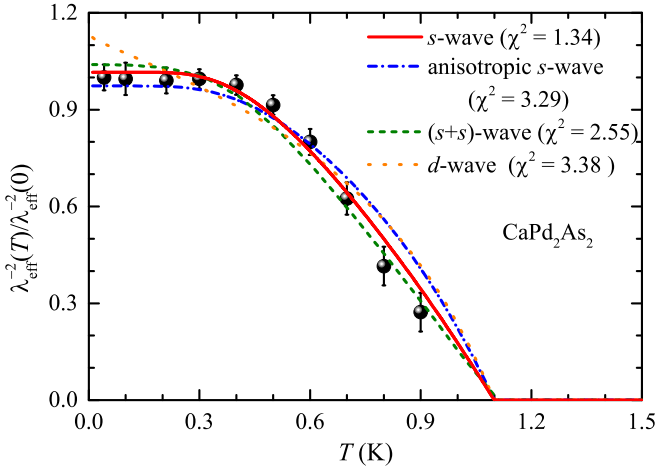

FIG. 5. Temperature T dependence of the inverse square of the normalized effective penetration depth $\lambda_{\rm eff}$ for $CaPd_2As_2$. The $\lambda_{\rm eff}^{-2}(T)/\lambda_{\rm eff}^{-2}(0)$ data were obtained using Eq. (4) and include all four-field sets of $\sigma_{\rm sc}(T, H)$. The solid red curve represents the fit for an isotropic single-gap s-wave model according to Eq. (5). The fits for anisotropic s-wave, two-gap $(s + s)$-wave and d-wave models are also shown.

where $f = [1 + \exp(E/k_{\rm B}T)]^{-1}$ is the Fermi function, and φ is the azimuthal angle along the Fermi surface. The T and φ dependent order parameter (superconducting energy gap) $\Delta(T, \varphi) = \Delta(0)\delta(T/T_c)g(\varphi)$ [51, 52] where $g(\varphi)$ contains the angle dependence of the superconducting gap structure, and $\delta(T/T_c)$ the T dependence. $g(\varphi) = 1$ for an isotropic s-wave gap, $g(\varphi) = |1 + \cos(4\varphi)|/2$ for an anisotropic s-wave gap, and $g(\varphi) = \cos(2\varphi)$ for a d-wave gap [51–53]. The T dependence of order parameter is approximated as $\delta(T/T_c) \approx \tanh[(1.82)(1.018(T_c/T - 1))^{0.51}]$ [54].

The solid red curve in Fig. 5 shows the fitting of $\lambda_{\rm eff}^{-2}(T)/\lambda_{\rm eff}^{-2}(0)$ with an isotropic s-wave model using the Eq. (5). We also fitted the $\lambda_{\rm eff}^{-2}(T)/\lambda_{\rm eff}^{-2}(0)$ with an anisotropic s-wave model, two-gap $(s + s)$-wave (isotropic) model and d-wave model which are also shown in Fig. 5. A closer inspection of the fits by the three models reflects that the single-gap isotropic s-wave model describes the T dependence of $\lambda_{\rm eff}$ the best. The lower value of goodness of fit parameter χ^2 (see Table I) also reflects the suitability of isotropic s-wave model over the

TABLE I. Parameters obtained from the fitting of $\lambda_{\rm eff}^{-2}(T)/\lambda_{\rm eff}^{-2}(0)$ for $CaPd_2As_2$ according to Eq. (5) using three models: single isotropic s-wave gap model, single anisotropic s-wave gap model, two isotropic $(s + s)$-wave gap model, and d-wave gap model.

Model	$\Delta_i(0)$ (meV)	$2\Delta(0)/k_{\rm B}T_c$	χ^2
isotropic s-wave	0.160(1)	3.37(3)	1.34
anisotropic s-wave	0.232(3)	4.89(8)	3.29
two gap $(s + s)$-wave	0.153(2), 0.041(1)	3.22(5), 0.86(4)	2.55
d-wave	0.266(2)	5.60(7)	3.38

anisotropic s-wave, $(s+s)$-wave and d-wave models. The values of the energy gaps obtained from the fits with different models are listed in Table I. We find an energy gap $\Delta(0) = 0.160(1)$ meV from the fit by the isotropic s-wave model which yields $2\Delta(0)/k_{\rm B}T_c = 3.37(3)$ ($T_c \approx 1.1$ K from μSR) which is little smaller than but close to the BCS theory value of 3.53 for single-band weak coupling isotropic s-wave symmetry. The value of gap estimated from our TF-μSR analyis is in good agreement with that estimated from the heat capacity ($\Delta(0) \approx 0.174$ meV) [30]. The jump in heat capacity at T_c gives a value $2\Delta(0)/k_{\rm B}T_c = 3.16$ for single crystal $CaPd_2As_2$ [30].

We notice that the analysis of TF-μSR reveals an isotropic superconducting gap structure in $CaPd_2As_2$. In the case of $CaPd_2Ge_2$ also μSR study revealed an isotropic superconducting gap structure [20]. In view of these observations, we are under the impression that a reduced values of $\Delta C_{\rm e}/\gamma_n T_{\rm c}$ (and corresponding $\Delta(0)/k_{\rm B}T_c$) does not necessarily imply an anisotropic superconducting gap structure as was initially conjectured from the reduced jump in electronic heat capacity at $T_{\rm c}$ and the analysis of the superconducting state electronic heat capacity with the α-model of BCS superconductivity [29–32].

The isotropic s-wave model fit also gives us an estimate of penetration depth which is found to be $\lambda_{\rm eff}(0) = 415(16)$ nm. This value is intermediate between the value of $\lambda_{\rm eff}(0) = 530 - 620$ nm estimated from the upper critical field and mean-free path length, and $\lambda_{\rm eff}(0) = 210(60)$ nm obtained from the penetration depth measurement using tunnel diode resonator (TDR) [30]. The higher value of $\lambda_{\rm eff}(0)$ compared to that obtained from TDR measurement [30] could be attributed to a lower value of mean free path on account of polycrystalline form of sample, and/or due to an underestimated depolarization rate $\sigma_{\rm TF}$. We estimate the superconducting carrier density $n_{\rm s}$ using the relation $n_{\rm s} = m^* c^2/4\pi\lambda_{\rm eff}(0)e^2$. Here we assume $n_{\rm s} \approx n_{\rm n}$, $n_{\rm n}$ being the normal state carrier density, see Refs. [55–57] for more details. The effective band mass $m^* = (1 + \lambda_{\rm e-ph})m_{\rm e}$ which is found to be $1.47\,m_{\rm e}$ ($m_{\rm e}$ being free electron mass) corresponding to the value of $\lambda_{\rm e-ph} = 0.47$ [30]. For $\lambda_{\rm eff}(0) = 415$ nm, we estimate $n_{\rm s} \approx 2.4 \times 10^{26}$ m^{-3}.

We thus see that while the analysis of TF μSR spectra reveals an isotropic s-wave superconductivity, the ZF μSR spectra reveal TRS breaking which is not expected for s-wave superconductor. Therefore in order to check whether $CaPd_2As_2$ lies into the category of a conventional superconductor or an unconventional superconductor according to Uemura plot [58, 59], we estimate the ratio of $T_c/T_{\rm F}$ where $T_{\rm F}$ is the Fermi temperature. According to Uemura plot, the value of ratio $T_c/T_{\rm F} \leq 0.001$ for a conventional SC, and lies between 0.01 to 0.1 for the unconventional SC. The $T_{\rm F}$ is estimated using the relation $k_{\rm B}T_{\rm F} = (\hbar^2/2m^*)(3\pi^2 n_{\rm s})^{2/3}$ [60]. For $n_{\rm s} \approx 2.4 \times 10^{26}$ m^{-3}, we get the value of $T_{\rm F} = 1110$ K and hence a ratio of $T_c/T_{\rm F} \approx 1/1000$ indicating that $CaPd_2As_2$ falls into the category of a conventional superconductor. The position of $CaPd_2As_2$ on Uemura plot of T_c versus $T_{\rm F}$ is shown in Fig. 6. This suggests that the TRS breaking in $CaPd_2As_2$ cannot be understood by the existing theories for TRS breaking in unconventional/multiband superconductors or superconductors having multi-orbital character of states at the Fermi level. A similar case was observed for the TRS breaking in $CaPd_2Ge_2$ [20] which also falls into the category of a conventional superconductor (see Fig. 6). In the case of $Sc_5Co_4Si_{10}$ [19] it is conjectured (based on the density functional theory calculations and group theoretical analysis) that the Fermi surface topography may favor the TRS breaking despite the conventional s-wave superconductivity. Whether a similar explanation can hold for TRS breaking in $CaPd_2Ge_2$ and $CaPd_2As_2$ remains to be examined.

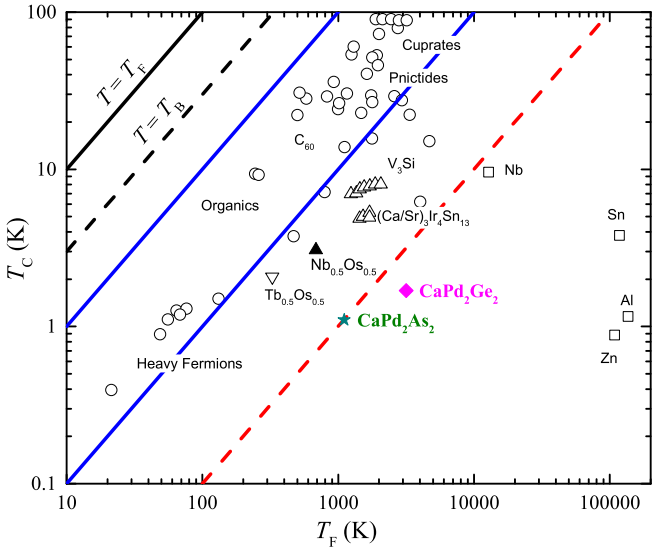

FIG. 6. The Uemura plot, depicting the superconducting T_c versus Fermi temperature $T_{\rm F}$ for various types of superconductors. The ratio $T_c/T_{\rm F}$ for unconventional superconductors lie between 0.01 to 0.1, i.e., between the solid blue lines. The conventional superconductors have $T_c/T_{\rm F} \leq 0.001$, i.e., on or right to the red dashed line. The positions of $CaPd_2As_2$ and $CaPd_2Ge_2$ on this plot classify them as conventional superconductors.

IV. CONCLUSIONS

We have investigated the time-reversal symmetry state and superconducting gap structure of an electron-phonon mediated s-wave superconductor $CaPd_2As_2$ by means of muon spin relaxation and rotation measurements. The μSR measurement confirms the bulk superconductivity in $CaPd_2As_2$ with a $T_c \approx 1.1$ K for the present polycrystalline sample. The ZF μSR provides clear evidence of time-reversal symmetry breaking in $CaPd_2As_2$. The analysis of ZF μSR spectra shows an increased value of relaxation rate $\lambda_{\rm ZF}$ in the superconducting state reveal-

ing the appearance of a spontaneous magnetic field associated with the TRS breaking upon entering the SC state. The Fourier transform of the TF μSR confirms a type-II superconductivity in $CaPd_2As_2$ consistent with the value of κ_{GL} estimated in an earlier work [30]. We analyzed the TF μSR spectra using a Gaussian oscillatory function and obtained the relaxation rate in superconducting state $\sigma_{sc}(T, H)$ which was then used to estimate the T dependent values of $\lambda_{\rm eff}$ using the Brandt method [46]. The analysis of $\lambda_{\rm eff}(T)$ reveals that it is best described by a single-band isotropic s-wave singlet gap structure with $2\Delta(0)/k_BT_c \approx 3.37$ consistent with the weak-coupling BCS superconductivity. Thus the TF μSR spectra reveals a weak-coupling s-wave superconductivity in $CaPd_2As_2$. The Uemura-plot classification based on the value of T_c/T_F also classifies $CaPd_2As_2$ to be a conventional superconductor. Therefore the occurrence of time-reversal symmetry breaking is quite striking. A similar TRS breaking was observed in our recent μSR study of Ge-analog $CaPd_2Ge_2$ [20]. Our findings should stimulate further experimental and theoretical works to understand the mechanism behind the TRS breaking in s-wave superconductors.

ACKNOWLEDGMENTS

DTA would like to thank the Royal Society of London for the Newton Advanced fellowship funding between UK and China, and the International Exchange funding between UK and Japan. DTA also thanks EPSRC UK (Grant number EP/W00562X/1) for funding. AB expresses gratitude to the Science and Engineering Research Board for the CRG Research Grants (CRG/2020/000698 & CRG/2022/008528) and CRS Project Proposal at UGC-DAE CSR (CRS/2021-22/03/549). We thank ISIS Facility for providing beam time RB1510100 [61].

[1] S. K. Ghosh, M. Smidman, T. Shang, J. F. Annett, A. D. Hillier, J. Quintanilla, and H. Yuan, Recent progress on superconductors with time-reversal symmetry breaking, J. Phys.: Condens. Matter **33**, 033001 (2021).
[2] S. K. Ghosh, J. F. Annett, and J. Quintanilla, Time-reversal symmetry breaking in superconductors through loop supercurrent order, New J. Phys. **23**, 083018 (2021).
[3] C. Kallin and J. Berlinsky, Chiral superconductors, Rep. Prog. Phys. **79**, 054502 (2016).
[4] T. Shang, M. Smidman, S. K. Ghosh, C. Baines, L. J. Chang, D. J. Gawryluk, J. A. T. Barker, R. P. Singh, D. M. Paul, G. Balakrishnan, E. Pomjakushina, M. Shi, M. Medarde, A. D. Hillier, H. Q. Yuan, J. Quintanilla, J. Mesot, and T. Shiroka, Time-reversal symmetry breaking in Re-based superconductors, Phys. Rev. Lett. **121**, 257002 (2018).
[5] D. Singh, J. Barker, A. Thamizhavel, D. M. Paul, A. Hillier, and R. Singh, Time-reversal symmetry breaking in the noncentrosymmetric superconductor Re_6Hf: Further evidence for unconventional behavior in the α-Mn family of materials, Phys. Rev. B **96**, 180501 (2017).
[6] D. Singh, K. P. Sajilesh, J. A. T. Barker, D. M. Paul, A. D. Hillier, and R. P. Singh, Time-reversal symmetry breaking in the noncentrosymmetric superconductor Re_6Ti, Phys. Rev. B **97**, 100505 (2018).
[7] R. P. Singh, A. D. Hillier, B. Mazidian, J. Quintanilla, J. F. Annett, D. M. Paul, G. Balakrishnan, and M. R. Lees, Detection of time-reversal symmetry breaking in the noncentrosymmetric superconductor Re_6Zr using muon-spin spectroscopy, Phys. Rev. Lett. **112**, 107002 (2014).
[8] G. M. Pang, Z. Y. Nie, A. Wang, D. Singh, W. Xie, W. B. Jiang, Y. Chen, R. P. Singh, M. Smidman, and H. Q. Yuan, Fully gapped superconductivity in single crystals of noncentrosymmetric Re_6Zr with broken time-reversal symmetry, Phys. Rev. B **97**, 224506 (2018).
[9] P. K. Biswas, H. Luetkens, T. Neupert, T. Stürzer, C. Baines, G. Pascua, A. P. Schnyder, M. H. Fischer, J. Goryo, M. R. Lees, H. Maeter, F. Brückner, H.-H. Klauss, M. Nicklas, P. J. Baker, A. D. Hillier, M. Sigrist, A. Amato, and D. Johrendt, Evidence for superconductivity with broken time-reversal symmetry in locally noncentrosymmetric SrPtAs, Phys. Rev. B **87**, 180503 (2013).
[10] A. D. Hillier, J. Quintanilla, and R. Cywinski, Evidence for time-reversal symmetry breaking in the noncentrosymmetric superconductor $LaNiC_2$, Phys. Rev. Lett. **102**, 117007 (2009).
[11] A. Bhattacharyya, D. T. Adroja, N. Kase, A. D. Hillier, A. M. Strydom, and J. Akimitsu, Unconventional superconductivity in the cage-type compound $Sc_5Rh_6Sn_{18}$, Phys. Rev. B **98**, 024511 (2018).
[12] A. Bhattacharyya, D. Adroja, N. Kase, A. Hillier, J. Akimitsu, and A. Strydom, Unconventional superconductivity in $Y_5Rh_6Sn_{18}$ probed by muon spin relaxation, Sci. Rep. **5**, 12926 (2015).
[13] A. Bhattacharyya, D. T. Adroja, J. Quintanilla, A. D. Hillier, N. Kase, A. M. Strydom, and J. Akimitsu, Broken time-reversal symmetry probed by muon spin relaxation in the caged type superconductor $Lu_5Rh_6Sn_{18}$, Phys. Rev. B **91**, 060503 (2015).
[14] D. Singh, M. S. Scheurer, A. D. Hillier, D. T. Adroja, and R. P. Singh, Time-reversal-symmetry breaking and unconventional pairing in the noncentrosymmetric superconductor La_7Rh_3, Phys. Rev. B **102**, 134511 (2020).
[15] D. A. Mayoh, A. D. Hillier, G. Balakrishnan, and M. R. Lees, Evidence for the coexistence of time-reversal symmetry breaking and Bardeen-Cooper-Schrieffer-like superconductivity in La_7Pd_3, Phys. Rev. B **103**, 024507 (2021).
[16] J. A. T. Barker, D. Singh, A. Thamizhavel, A. D. Hillier, M. R. Lees, G. Balakrishnan, D. M. Paul, and R. P. Singh, Unconventional superconductivity in La_7Ir_3 revealed by muon spin relaxation: Introducing a new family of noncentrosymmetric superconductor that breaks time-reversal symmetry, Phys. Rev. Lett. **115**, 267001 (2015).
[17] T. Shang, S. K. Ghosh, J. Z. Zhao, L.-J. Chang, C. Baines, M. K. Lee, D. J. Gawryluk, M. Shi,

M. Medarde, J. Quintanilla, and T. Shiroka, Time-reversal symmetry breaking in the noncentrosymmetric Zr_3Ir superconductor, Phys. Rev. B **102**, 020503 (2020).
[18] T. Shang, M. Smidman, A. Wang, L.-J. Chang, C. Baines, M. K. Lee, Z. Y. Nie, G. M. Pang, W. Xie, W. B. Jiang, M. Shi, M. Medarde, T. Shiroka, and H. Q. Yuan, Simultaneous nodal superconductivity and time-reversal symmetry breaking in the noncentrosymmetric superconductor CaPtAs, Phys. Rev. Lett. **124**, 207001 (2020).
[19] A. Bhattacharyya, M. R. Lees, K. Panda, P. P. Ferreira, T. T. Dorini, E. Gaudry, L. T. F. Eleno, V. K. Anand, J. Sannigrahi, P. K. Biswas, R. Tripathi, and D. T. Adroja, Nodeless time-reversal symmetry breaking in the centrosymmetric superconductor $Sc_5Co_4Si_{10}$ probed by muon-spin spectroscopy, Phys. Rev. Mater. **6**, 064802 (2022).
[20] V. K. Anand, A. Bhattacharyya, D. T. Adroja, K. Panda, P. K. Biswas, A. D. Hillier, and B. Lake, Time-reversal symmetry breaking and *s*-wave superconductivity in $CaPd_2Ge_2$: A μSR study, Phys. Rev. B **108**, 224519 (2023).
[21] P. K. Biswas, S. K. Ghosh, J. Z. Zhao, D. A. Mayoh, N. Zhigadlo, X. Xu, C. Baines, A. Hillier, G. Balakrishnan, and M. R. Lees, Chiral singlet superconductivity in the weakly correlated metal $LaPt_3P$, Nature Commun. **12**, 2504 (2021).
[22] A. D. Hillier, J. Quintanilla, B. Mazidian, J. F. Annett, and R. Cywinski, Nonunitary triplet pairing in the centrosymmetric superconductor $LaNiGa_2$, Phys. Rev. Lett. **109**, 097001 (2012).
[23] T. Shang, S. Ghosh, J. Zhao, L.-J. Chang, C. Baines, M. Lee, D. J. Gawryluk, M. Shi, M. Medarde, J. Quintanilla, *et al.*, Time-reversal symmetry breaking in the noncentrosymmetric Zr_3Ir superconductor, Phys. Rev. B **102**, 020503 (2020).
[24] A. Bhattacharyya, P. Ferreira, K. Panda, S. Masunaga, L. R. de Faria, L. E. Correa, F. B. Santos, D. T. Adroja, K. Yokoyama, T. T. Dorini, R. F. Jardim, L. T. F. Eleno, and A. J. S. Machado, Electron-phonon superconductivity in C-doped topological nodal-line semimetal Zr_5Pt_3: A muon spin rotation and relaxation (μSR) study, J. Phys.: Condens. Matter **34**, 035602 (2021).
[25] G. M. Luke, Y. Fudamoto, K. M. Kojima, M. I. Larkin, J. Merrin, B. Nachumi, Y. J. Uemura, Y. Maeno, Z. Q. Mao, Y. Mori, H. Nakamura, and M. Sigrist, Time-reversal symmetry-breaking superconductivity in Sr_2RuO_4, Nature **394**, 558 (1998).
[26] G. M. Luke, Y. Fudamoto, K. M. Kojima, M. I. Larkin, B. Nachumi, Y. J. Uemura, J. E. Sonier, Y. Maeno, Z. Q. Mao, Y. Mori, and D. F. Agterberg, Unconventional superconductivity in Sr_2RuO_4, Physica B: Condens. Matter **289–290**, 373 (2000).
[27] V. Grinenko, S. Ghosh, R. Sarkar, J.-C. Orain, A. Nikitin, M. Elender, D. Das, Z. Guguchia, F. Brückner, M. E. Barber, J. Park, N. Kikugawa, D. A. Sokolov, J. S. Bobowski, T. Miyoshi, Y. Maeno, A. P. Mackenzie, H. Luetkens, C. W. Hicks, and H.-H. Klauss, Split superconducting and time-reversal symmetry-breaking transitions, and magnetic order in Sr_2RuO_2 under uniaxial stress, Nat. Phys. **17**, 748 (2021).
[28] B. J. Wilson and M. P. Das., Time-reversal-symmetry-broken state in the bcs formalism for a multi-band superconductor, Phys. Rev. Lett. **112**, 107002 (2014).
[29] V. K. Anand, H. Kim, M. A. Tanatar, R. Prozorov, and D. C. Johnston, Superconductivity and physical properties of $CaPd_2Ge_2$ single crystals, J. Phys.: Condens. Matter **26**, 405702 (2014).
[30] V. K. Anand, H. Kim, M. Tanatar, R. Prozorov, and D. Johnston, Superconducting and normal-state properties of APd_2As_2 (A= Ca, Sr, Ba) single crystals, Phys. Rev. B **87**, 224510 (2013).
[31] H. Padamsee, J. Neighbor, and C. Shiffman, Quasiparticle phenomenology for thermodynamics of strong-coupling superconductors, J. Low Temp. Phys. **12**, 387 (1973).
[32] D. C. Johnston, Elaboration of the α-model derived from the bcs theory of superconductivity, Supercond. Sci. Technol. **26**, 115011 (2013).
[33] Q.-P. Ding, P. Wiecki, V. Anand, N. Sangeetha, Y. Lee, D. Johnston, and Y. Furukawa, Volovik effect and fermi-liquid behavior in the s-wave superconductor $CaPd_2As_2$: ^{75}As NMR-NQR measurements, Phys. Rev. B **93**, 140502 (2016).
[34] I. A. Nekrasov and M. V. Sadovskii, Comparative study of electronic structure of new superconductors (Sr, Ca)Pd_2As_2 and related compound $BaPd_2As_2$, JETP Lett. **98**, 24 (2013).
[35] I. R. Shein, S. L. Skornyakov, V. I. Anisimov, and A. L. Ivanovskii, Elastic and electronic properties of superconducting $CaPd_2As_2$ and $SrPd_2As_2$ vs. non-superconducting $BaPd_2As_2$, J. Supercond. Nov. Magn. **27**, 155 (2014).
[36] V. K. Anand, P. K. Perera, A. Pandey, R. J. Goetsch, A. Kreyssig, and D. C. Johnston, Crystal growth and physical properties of $SrCu_2As_2$, $SrCu_2Sb_2$, and $BaCu_2Sb_2$, Phys. Rev. B **85**, 214523 (2012).
[37] J. Rodríguez-Carvajal, Recent advances in magnetic structure determination by neutron powder diffraction, Physica B: Condens. Matter **192**, 55 (1993).
[38] W. K. Hofmann and W. Jeitschko, Ternäre palladiumpnictide der erdalkali-und seltenen erdmetalle mit $ThCr_2Si_2$-und $CaBe_2Ge_2$-struktur, Monatsh. Chem. **116**, 569 (1985).
[39] S. L. Lee, R. Cywinski, and S. Kilcoyne, *Muon science: Muons in physics, chemistry and materials*, Vol. 51 (CRC press, 1999).
[40] F. L. Pratt, WIMDA: A muon data analysis program for the windows PC, Physica B: Condens. Matter **289**, 710 (2000).
[41] A. Bhattacharyya, D. Adroja, J. Lord, L. Wang, Y. Shi, K. Panda, H. Luo, and A. Strydom, Quantum fluctuations in the quasi-one-dimensional non-fermi liquid system $CeCo_2Ga_8$ investigated using μSR, Phys. Rev. B **101**, 214437 (2020).
[42] A. Bhattacharyya, K. Panda, D. Adroja, N. Kase, P. K. Biswas, S. Saha, T. Das, M. R. Lees, and A. D. Hillier, Investigation of superconducting gap structure in HfIrSi using muon spin relaxation/rotation, J. Phys.: Condens. Matter **32**, 085601 (2019).
[43] R. S. Hayano, Y. J. Uemura, J. Imazato, N. Nishida, K. Nagamine, T. Yamazaki, Y. Ishikawa, and H. Yasuoka, Spin fluctuations of itinerant electrons in mnsi studied by muon spin rotation and relaxation, J. Phys. Soc. Jpn. **49**, 1773 (1980).
[44] K. Panda, A. Bhattacharyya, P. N. Ferreira, R. Mondal, A. Thamizhavel, D. T. Adroja, C. Heil, L. T. F. Eleno,

and A. D. Hillier, Probing the superconducting gap structure of ScRuSi via μSR and first-principles calculations, Physical Review B **109**, 224517 (2024).

[45] E. Brandt, Magnetic field density of perfect and imperfect flux line lattices in type II superconductors. I. application of periodic solutions, J. Low Temp. Phys. **73**, 355 (1988).

[46] E. H. Brandt, Properties of the ideal ginzburg-landau vortex lattice, Phys. Rev. B **68**, 054506 (2003).

[47] K. Panda, A. Bhattacharyya, D. T. Adroja, N. Kase, P. K. Biswas, S. Saha, T. Das, M. R. Lees, and A. D. Hillier, Probing the superconducting ground state of ZrIrSi: A muon spin rotation and relaxation study, Phys. Rev. B **99**, 174513 (2019).

[48] A. Bhattacharyya, D. Adroja, K. Panda, S. Saha, T. Das, A. Machado, O. Cigarroa, T. Grant, Z. Fisk, A. Hillier, and P. Manfrinetti, Evidence of a Nodal Line in the Superconducting Gap Symmetry of Noncentrosymmetric $ThCoC_2$, Physical Review Letters **122**, 147001 (2019).

[49] R. Prozorov and R. W. Giannetta, Magnetic penetration depth in unconventional superconductors, Superconductor Science and Technology **19**, R41 (2006).

[50] A. Bhattacharyya, D. T. Adroja, A. K. Jana, K. Panda, P. P. Ferreira, Y. Zhao, T. Ying, H. Hosono, T. T. Dorini, L. T. F. Eleno, P. K. Biswas, G. Stenning, R. Tripathi, and Y. Qi, Exploring superconductivity in $Ba_3Ir_4Ge_{16}$: Experimental and theoretical insights, J. Alloys Comp. **978**, 173374 (2024).

[51] J. F. Annett, Symmetry of the order parameter for high-temperature superconductivity, Adv. Phys. **39**, 83 (1990).

[52] G. M. Pang, M. Smidman, W. B. Jiang, J. K. Bao, Z. F. Weng, Y. F. Wang, L. Jiao, J. L. Zhang, G. H. Cao, and H. Q. Yuan, Evidence for nodal superconductivity in quasi-one-dimensional $K_2Cr_3As_3$, Phys. Rev. B **91**, 220502 (2015).

[53] R. Khasanov, K. Conder, E. Pomjakushina, A. Amato, C. Baines, Z. Bukowski, J. Karpinski, S. Katrych, H.-H. Klauss, H. Luetkens, A. Shengelaya, and N. D. Zhigadlo, Evidence of nodeless superconductivity in $FeSe_{0.85}$ from a muon-spin-rotation study of the in-plane magnetic penetration depth, Phys. Rev. B **78**, 220510 (2008).

[54] A. Carrington and F. Manzano, Magnetic penetration depth of MgB_2, Physica C: Superconductivity **385**, 205 (2003).

[55] A. D. Hillier and R. Cywinski, The classification of superconductors using muon spin rotation, Applied Magnetic Resonance **13**, 95 (1997).

[56] V. K. Anand, A. D. Hillier, D. T. Adroja, A. M. Strydom, H. Michor, K. A. McEwen, and B. D. Rainford, Specific heat and μSR study on the noncentrosymmetric superconductor $LaRhSi_3$, Phys. Rev. B **83**, 064522 (2011).

[57] D. T. Adroja, A. Bhattacharyya, Y. J. Sato, M. R. Lees, P. K. Biswas, K. Panda, V. K. Anand, G. B. G. Stenning, A. D. Hillier, and D. Aoki, Pairing symmetry of an intermediate valence superconductor measurements, Physical Review B **103**, 104514 (2021).

[58] Y. J. Uemura, G. M. Luke, B. J. Sternlieb, J. H. Brewer, J. F. Carolan, W. N. Hardy, R. Kadono, J. R. Kempton, R. F. Kiefl, S. R. Kreitzman, P. Mulhern, T. M. Riseman, D. L. Williams, B. X. Yang, S. Uchida, H. Takagi, J. Gopalakrishnan, A. W. Sleight, M. A. Subramanian, C. L. Chien, M. Z. Cieplak, G. Xiao, V. Y. Lee, B. W. Statt, C. E. Stronach, W. J. Kossler, and X. H. Yu, Universal correlations between T_c and $\frac{n_s}{m^*}$ (carrier density over effective mass) in high-T_c cuprate superconductors, Phys. Rev. Lett. **62**, 2317 (1989).

[59] Y. Uemura, Classifying superconductors in a plot of T_c versus fermi temperature T_F, Physica C: Superconductivity **185**, 733 (1991).

[60] C. Kittel, *Introduction to Solid State Physics* (John Wiley & Sons, Inc., 2005).

[61] V. K. Anand, D. T. Adroja, and A. D. Hillier, Study of superconductivity in $CaPd_2As_2$, $SrPd_2As_2$ and $CaPd_2Ge_2$ using muon spin relaxation and rotation (2015).